

Wave-cascades in wavy flows

Inertia-gravity wave emission from baroclinic waves: DNS and lab experiments

U. Harlander, S. Abide, S. Viazzo, I. Raspo, A. Randriamampianina, Dept. Aerodynamics and Fluid Mechanics, Brandenburg University of Technology (BTU) Cottbus-Senftenberg

In Short

- Which role plays the heat transfer at the upper free boundary for inertia-gravity wave (IGW) emission?
- Does the IGW emission depend on the radial ('north-south') temperature difference?
- How does low-frequency variability influence the IGW emission and is there intermittency?
- To answer these questions a fast DNS code is mandatory to do long term simulations and compare them with experimental data.

□ **Context** Inertia-gravity waves (IGWs) play a fundamental role for the energy and momentum transport from the troposphere into the middle atmosphere where the waves drive the global circulation. These waves have wavelength far below 100km and are part of the subgrid-scale processes that need to be parameterized in weather and climate models. Therefore, all aspects of IGW generation in the atmosphere need to be understood. One of the least understood aspects is the emission of IGWs from jet and front systems in the atmosphere. Although many studies have established the importance of these non-orographic sources, the mechanisms responsible for wave emissions are still not fully clear. The complexity of the three-dimensional flow pattern, where a large number of interacting processes occur, and distribution of the sources over large areas point towards the need for laboratory experiments and idealised numerical simulations. Fig. 1 gives the experimental setup at BTU C-S used to study multiscale wave processes [1,2].

□ **Problematic** The baroclinic tank cavity as set up in Cottbus is such idealization of the systems of jets and fronts in the atmosphere. Recent comparisons with DNS suggest a certain bias which could be introduced at the free surface. The omission of heat transfer and evaporative cooling might be a source of noticeable discrepancies between experiments and simulations. Therefore, the emission mechanisms of IGWs should be interpreted this type of effect in account. Direct numerical simulations is appealing to predict flows with perfect control of idealized operating conditions, at least if the

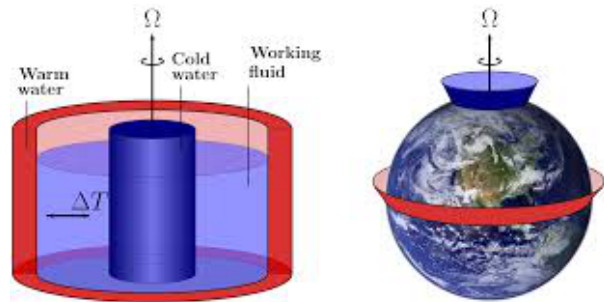


Figure 1: Sketch of the baroclinic wave tank experiment at BTU Cottbus-Senftenberg (left) and correspondence between the cylindrical geometry of the experiment and the Earth atmosphere (right).

uncertainties associated with numerical methods are avoided. However, the presence of large-scale baroclinic waves and small-scale IGWs makes use of direct numerical simulations challenging to simulate this multi-scale flow [3,4].

In order to provide insights on the emission IGWs from jets and fronts, we propose to perform direct numerical simulations of the laboratory experiments performed at BTU-CS. Particular attention is paid to the free surface by relying on laboratory experiments. In order to carry out long-term direct numerical simulations of the baroclinic wave, the time of simulations has to remain reasonable. We have therefore based this project on a solver that combines the higher-resolution capability of compact schemes and spectral methods with high-performance computing.

□ **Numerical methods** The Navier-Stokes equations expressed in cylindrical coordinates system and in a rotating frame of rotation rate Ω are considered. The configuration of the baroclinic cavity is sketched fig. 1. The governing equations are solved for the velocity \mathbf{u} , the pressure p , and the temperature T , being discretized with a mixed Fourier-Galerkin/compact schemes or a Fourier-Galerkin/spectral methods in space. A semi-implicit fractional step method is considered for the time advancement. This reduces the solution of the Navier-Stokes equations to solutions of the Helmholtz/Poisson equations and simplifies the calculation of space derivatives and interpolations [6]. The parallel strategy of our code depends on the local or global nature of the space approximation.

□ **High Performance Computing** Due to the global nature of higher-order discretization, specific parallel strategies need to be specifically designed.

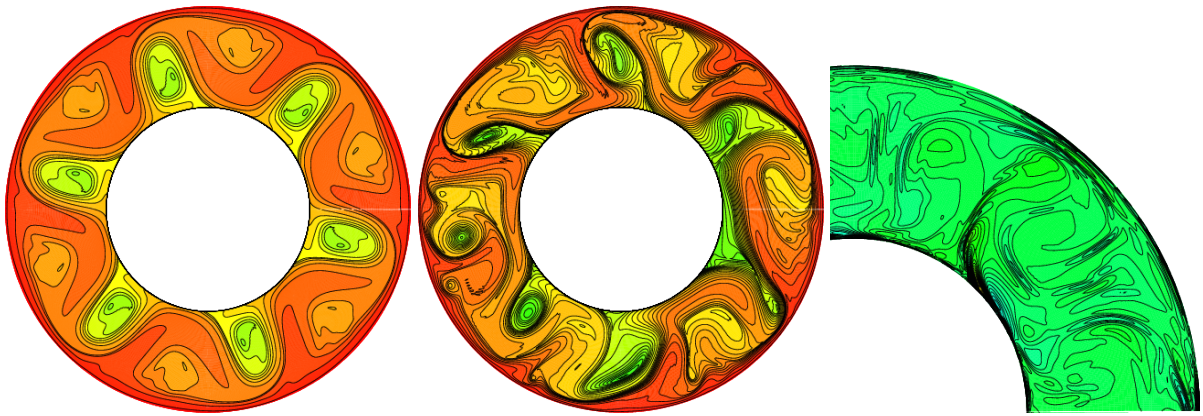


Figure 2: Baroclinic waves for the non-axisymmetric regular $\Omega = 0.6 \text{ rpm}$ (left) and irregular $\Omega = 1.0 \text{ rpm}$ (middle) regimes. Isocontour of the temperature surface: 40 uniformly distributed isovalues for $\Delta T = 4, K$. Horizontal divergence isocontour (right): 40 uniformly distributed isovalues for $\|\nabla_h \mathbf{u}\| \leq 0.04 \text{ ms}^{-2}$.

Thus, the computation of derivatives and interpolations with compact fourth-order schemes is based on parallelization using halo communication (neighbour to neighbour). This strategy is called rPDD and has been analysed in [5] for the solution of an incompressible fluid flow. The solution of the Helmholtz/Poisson equations and the spectral calculation of the derivatives are based on global approximations. In this case, the pencil decomposition strategy [7] is used for an efficient and "user friendly" parallelization.

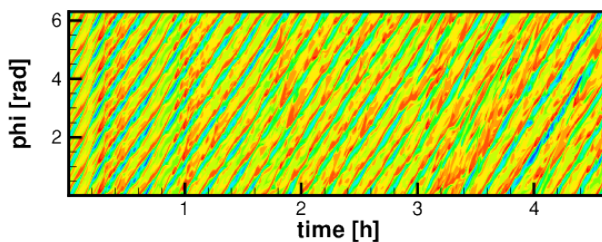


Figure 3: Hovmöller plot of the temperature at the vicinity of the free flow surface ($\Omega = 1 \text{ rpm}, \Delta T = 4 K$).

□ **Preliminary results** A coarse-DNS of mesh size $(N_\phi \times N_z \times N_r) = 1024 \times 96 \times 128$ has been carried out to reproduce a regular wavy and an irregular regime already observed with the baroclinic cavity set-up of BTU C-S. The irregular regime occurs for a rotation rate to $\Omega = 1 \text{ rpm}$ with a $4 K$ horizontal temperature gradient. The simulation has been initialized using previous data from an experiment with a rotation rate $\Omega = 0.6 \text{ rpm}$. The temperature at the top lid of the cavity is shown fig. 2 for these two regimes. The slice of the horizontal divergence shown in fig. 2 illustrates the multi-scale phenomena inherent to the baroclinic wave dynamics. The computational challenge of the long-term simulation is illustrated in fig. 3. The Hovmöller plot of the surface temperature suggests that the transition to the irregular regime begins to occur after a long integration time.

WWW

<http://www.uharlander.csww.de/>

More Information

- [1] C. Rodda, S. Hien, U. Achatz, U. Harlander, *Exp. Fluids* **61**, (2020). doi:10.1007/s00348-019-2825-z
- [2] C. Rodda, U. Harlander, *J. Atmos. Sci.* **77**, (2020). doi:10.1175/JAS-D-20-0033.1
- [3] T. Von Larcher, S. Viazzo, U. Harlander, M. Vincze, A. Randriamampianina, *J. Fluid Mech.* **841**, (2018). doi:10.1017/jfm.2018.10
- [4] S. Hien, J. Rolland, S. Borchert, L. Schoon, C. Zülicke, U. Achatz, *J. Fluid Mech.* **838**, (2018). doi:10.1017/jfm.2017.883
- [5] S. Abide, M.S. Binous, B. Zeghmami, *Int. J. Comput. Fluid Dyn.* **31**, (2017). doi:10.1080/10618562.2017.1326592
- [6] S. Abide, S. Viazzo, I. Raspo, A. Randriamampianina, *Comput. Fluids* **174**, (2018). doi:10.1016/j.compfluid.2018.07.016
- [7] <http://www.2decomp.org/>

Project Partners

Univ Aix Marseille, M2P2; Univ Perpignan Via Domitia, LAMPS

Funding

This project is funded by DAAD and MEAE/MESRI in the frame of a PROCOPE (PHC 46672RE)